0888-8809/07/$15.00/0
Printed in U.S.A.

Molecular Endocrinology 21(1):30–48

doi: 10.1210/me.2006-0072

The Use of *in Vitro* Peptide Binding Profiles and *in Silico* Ligand-Receptor Interaction Profiles to Describe Ligand-Induced Conformations of the Retinoid X Receptor α Ligand-Binding Domain

Simon Folkertsma, Paula I. van Noort, Arnold de Heer, Peter Carati, Ralph Brandt, Arie Visser, Gerrit Vriend, and Jacob de Vlieg

Centre for Molecular and Biomolecular Informatics (S.F., G.V., J.d.V.), University of Nijmegen, 6500 GL Nijmegen, The Netherlands; and Organon NV (P.I.v.N., A.d.H., P.C., R.B., A.V., J.d.V.), 5340 BH Oss, The Netherlands

It is hypothesized that different ligand-induced conformational changes can explain the different interactions of nuclear receptors with regulatory proteins, resulting in specific biological activities. Understanding the mechanism of how ligands regulate cofactor interaction facilitates drug design. To investigate these ligand-induced conformational changes at the surface of proteins, we performed a time-resolved fluorescence resonance energy transfer assay with 52 different cofactor peptides measuring the ligand-induced cofactor recruitment to the retinoid X receptor-α (RXRα) in the presence of 11 compounds. Simultaneously we analyzed the binding modes of these compounds by molecular docking. An automated method converted the complex three-dimensional data of ligand-protein interactions into two-dimensional fingerprints, the so-called ligand-receptor interaction profiles. For a subset of compounds the conformational changes at the surface, as measured by peptide recruitment, correlate well with the calculated binding modes, suggesting that clustering of ligand-receptor interaction profiles is a very useful tool to discriminate compounds that may induce different conformations and possibly different effects in a cellular environment. In addition, we successfully combined ligand-receptor interaction profiles and peptide recruitment data to reveal structural elements that are possibly involved in the ligand-induced conformations. Interestingly, we could predict a possible binding mode of LG100754, a homodimer antagonist that showed no effect on peptide recruitment. Finally, the extensive analysis of the peptide recruitment profiles provided novel insight in the potential cellular effect of the compound; for the first time, we showed that in addition to the induction of coactivator peptide binding, all well-known RXRα agonists also induce binding of corepressor peptides to RXRα. (*Molecular Endocrinology* 21: 30–48, 2007)

THE COMMUNICATION BETWEEN different functional sites of a protein is essential in the regulation of the various activities commonly displayed by each protein. The biological response in the cell is not defined by the activity of each of the different functional sites in the protein separately, but from the effective coupling of those diverse signals. The nuclear receptor (NR) ligand-binding domain (LBD) is well suited to the study of this communication because this domain has three distinct functional sites: 1) the ligand-binding pocket (LBP) that accommodates the ligand; 2) the cofactor binding groove that facilitates binding of (de)activating regulatory proteins; and 3) the dimerization interface that allows for the interaction with other NRs. The LBD is a module of the full-length NR, which is a ligand-activated transcription factor with a common architecture (1–3). NRs consist of an N-terminal domain that contains the ligand-independent activation function 1 (AF-1), a central DNA-binding domain and a C-terminal LBD that harbors the important ligand-dependent activation function 2 (AF-2). In general, NRs are activated by binding of an agonist in the LBP of the LBD, which leads to stabilization of the AF-2 helix [also called helix 12 (H12)] in the agonist position (4–6). The movement of H12 facilitates the formation of the cofactor binding groove (7). Coactivators bind into this groove with a short helix that

First Published Online October 12, 2006

Abbreviations: AF, Activation function; ARES, automatic residue extraction system; 9-*cis* RA, 9-*cis* retinoic acid; 3D, three-dimensional; DHA, docosa hexaenoic acid; ER, estrogen receptor; GST, glutathione *S*-transferase; H12, helix 12; LBD, ligand binding domain; LBP, ligand binding pocket; MI, modulation index; MD, molecular dynamics; NCoR, nuclear receptor corepressor; NR, nuclear receptor; PDA, pentadecanoic acid; RAR, retinoic acid receptor; RIP, receptor-interacting protein; RXR, retinoid X receptor; SMRT, silencing mediator of retinoid and thyroid hormone receptor; SNRM, selective nuclear receptor modulator; SRC, steroid receptor coactivator; TR-FRET, time-resolved fluorescence resonance energy transfer; TTNPB, 4-[(E)-2-(5,6,7,8-tetrahydro-5,5,8,8-tetramethyl-2-napthalenyl-1-propenyl] benzoic acid.

***Molecular Endocrinology* is published monthly by The Endocrine Society (http://www.endo-society.org), the foremost professional society serving the endocrine community.**

contains a LXXLL sequence motif (NR box) (7–9). In contrast, an antagonist displaces H12, resulting in the dissociation of coactivators and the association of corepressors. Corepressors bind into the cofactor binding groove similarly to coactivators, but with a LXX(I/H)IXXX(I/L) sequence motif (10–12). The only available crystal structure with a corepressor shows that the corepressor peptide position is slightly tilted so that it partially overlaps with the agonistic location of H12 (10). Subsequently, the receptor-cofactor complex binds as a homodimer, heterodimer, or monomer to NR-specific response elements in the promoter region of target genes, which results in up- or down-regulation of those genes.

The above described mechanism suggests that agonists and antagonists induce two distinct conformational states of the LBD, *i.e*. stabilizing H12 in the agonist or antagonist position, respectively. These distinct conformations lead to the interaction with coactivators or corepressors and result in two distinct patterns of gene expression. However, it was observed that different agonists induce different gene expression profiles (13, 14). This may suggest that H12 does not have two distinct positions but can take any preferential position between the distinct agonist position and antagonist position. It is the combination of both compound and cofactor that determines the position of H12 and therefore the effect on gene expression. This suggests the existence of a more subtle communication pathway between the LBP and the cofactor binding groove of the NR. It has been shown for the estrogen receptor (ER) α and the peroxisome proliferator-activated receptor-γ (13, 15) that the binding of different ligands results in distinct patterns of cofactor binding. The cofactors in those studies are mimicked by helical peptides of 20–25 amino acids, containing the LXXLL coactivator motif or the LXX(I/H)IXXX(I/L) corepressor motif. These different patterns of peptide binding, so-called peptide recruitment profiles, are most likely caused by different conformations at the NR surface, in particular the cofactor binding groove. These studies show that peptide recruitment profiles are very useful to probe the conformation at the NR surface and to study the position of H12 in the presence of ligand and cofactor peptides. Moreover, compounds can be clustered according to their similarity in peptide recruitment profiles. It is believed that compounds in one peptide recruitment cluster induce similar conformations at the NR surface, which may result in transcription of the same set of target genes. From a structure-based drug design perspective it is therefore important to know which interactions between ligand and receptor cause a specific NR surface conformation, *i.e*. peptide recruitment profile. In other words, molecular understanding of the communication between LBP and cofactor binding groove may be one step further toward the design of NR drugs with a certain gene transcription profile.

In this paper we describe a methodology that helps to obtain this molecular understanding of ligand-induced conformations of the NR surface. We first measured peptide recruitment profiles for a set of different ligands. Second, we studied whether these different ligands actually have distinct binding modes using the available X-ray structures and docking. The different binding modes of compounds were represented by so-called ligand-receptor interaction profiles, thereby converting complex three dimensional (3D) data into two-dimensional fingerprints. These ligand-receptor interaction profiles were used to cluster compounds that bind in a similar manner. Finally we compared the clusters of the peptide recruitment profiles with the clusters of the ligand-receptor interaction profiles to reveal residue positions that are involved in signaling between the LBP and the surface of the LBD.

As a representative of the NRs we used the retinoid X receptor (RXR) α. RXRs (16) are unique within the NR superfamily because they form heterodimers with many other NRs and also function autonomously, as homodimers (17). The receptors are involved in important processes such as the regulation of carbohydrate and lipid metabolism, cell differentiation, proliferation, and morphogenesis. RXRs are regulated by retinoids, which are derivatives of vitamin A. The natural ligand of these receptors is 9-*cis* retinoic acid (9-*cis* RA) (18). Another class of RXR ligands comprises fatty acids, *e.g*. oleic acid, docosa hexaenoic acid (DHA), and phytanic acid (19–21). Finally, there are many synthetic ligands known for RXR (22), some of which are currently available as drugs for the treatment of (skin) cancers and dermatological diseases, such as psoriasis and acne.

In this study the induced peptide recruitment profiles of 10 well-described RXR ligands [and one retinoic acid receptor (RAR) ligand, TTNPB] were determined using a time-resolved fluorescence resonance energy transfer (TR-FRET) assay with 52 peptides. Simultaneously, the binding modes of these ligands in the pocket of RXRα were determined by modeling and molecular dynamics (MD) simulations. Clustering of the peptide recruitment profiles revealed that the compounds induced three distinct conformations at the surface of the LBD. Clustering of the binding modes showed two distinct modes of ligand binding for the RXR compounds. We successfully combined ligand binding profiles and peptide recruitment profiles to reveal structural determinants of signaling from the LBP to the surface of the LBD.

RESULTS

To investigate whether different RXR ligands induce different conformations at the RXRα LBD surface, we performed a peptide recruitment assay with 52 peptides (10^{-7} M) and 11 different ligands (10^{-5} M). The resulting peptide recruitment profiles are depicted in Fig. 1. Figure 1A shows the raw fluorescence intensity data. This figure shows that approximately half of the

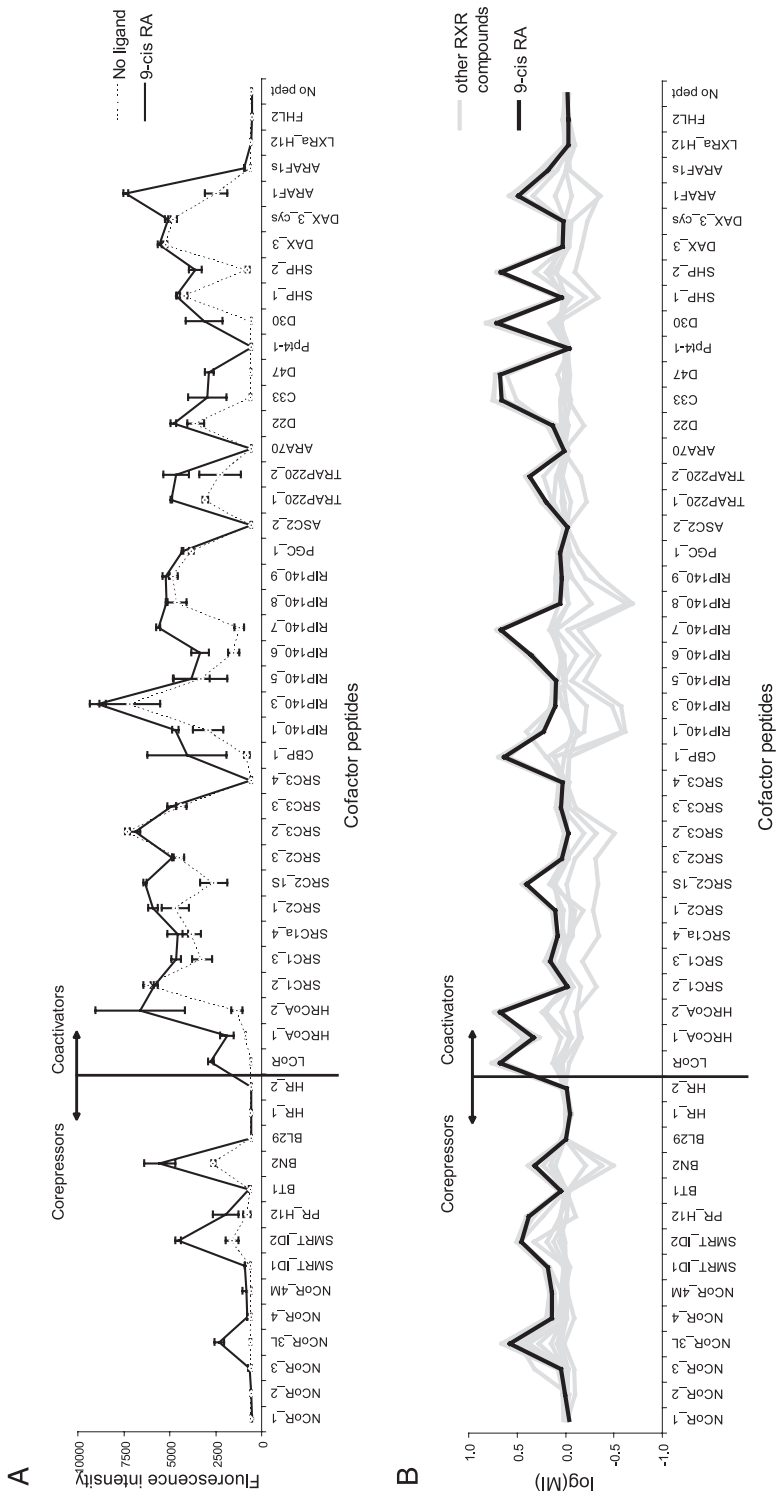

Fig. 1. Peptide Recruitment Profiles of RXRα LBD Induced by Different Ligands

A, Binding of 52 biotinylated peptides (0.1 μM) to GST-labeled hRXRα LBD (10 nM) in the absence (*dotted line*) and presence of 10 μM 9-*cis* RA (*solid line*). The SEM of two separate experiments, each performed in duplicate, is indicated by the *error bars*. B, Peptide recruitment profiles of 11 RXR ligands: the association and dissociation of 52 peptides to hRXRα LBD is represented as log(MI) values. The modulation index (MI) was obtained by dividing the fluorescence intensity in the presence of ligand by the intensity in the absence of ligand. Each *line* represents the average peptide recruitment profile for one of the 11 compounds. The SEM for each profile is given in supplemental Fig. 1 published as supplemental data on The Endocrine Society's Online Journals web site. The average peptide recruitment profile of 9-*cis* RA is highlighted as a *black solid line*. Peptides have been divided in coactivators or corepressors on the basis of their sequence motif.

peptides already bind to the RXRα surface in the absence of ligand (*dotted line*). The majority of these peptides are derived from coactivators. This suggests that H12 is stabilized in the agonist position in the absence of ligand, which is also observed in several NR LBD apo crystal structures (*e.g*. Refs. 23–27). Most likely, these peptides bind so well in the cofactor binding groove that they stabilize H12 in the agonist position (and *vice versa*). Figure 1A also shows the peptide recruitment profile in the presence of 9-*cis* RA, the natural ligand of RXRα (*solid line*). For many peptides, the fluorescence intensity, which is a measure of the peptide binding to the LBD, is higher in the presence of 9-*cis* RA. This indicates that the affinity of these peptides is increased due to the binding of 9-*cis* RA in the LBP.

Because the basal ligand-independent signal varies between different peptides, it is difficult to easily compare the effect of the ligand. For this purpose, the log[modulation index (MI)] was calculated (see *TR-FRET Assay* in *Materials and Methods* for more details), and the resulting peptide recruitment profile of 9-*cis* RA is depicted in Fig. 1B (*black line*). This representation directly shows whether a compound is associative or dissociative. Values above zero indicate recruitment of peptides, and thus an associative effect of the ligand on peptide binding. In contrast, values below zero indicate dissociation of peptides and therefore a dissociative effect of the compound on peptide binding. A log(MI) value of approximately zero means that the peptide does not bind or that the binding of a peptide is hardly changed by the ligand.

Peptides that Do Not Bind in the Absence and Presence of 9-*cis* RA

The peptide recruitment profile of 9-*cis* RA in Fig. 1B (*dark line*) shows that 25 peptides have a log(MI) value of approximately zero (log(MI) <0.1). Of these 25 peptides, 12 also do not bind in the absence of 9-*cis* RA (Fig. 1A), indicating that these peptides are not compatible with the RXRα cofactor binding groove. These 12 peptides include six peptides with a corepressor motif (NcoR_1, NCoR_2, BL29, HR_1, HR_2, BT_1) and six peptides with a coactivator motif (SRC3_4, ASC2_2, ARA70, Ppt4–1, LXRα_H12, and FHL2). A sequence alignment of the six nonbinding corepressor peptides revealed no sequence similarity that explains why these peptides do not bind (data not shown). The alignment of the six nonbinding coactivator peptides (Fig. 2A) showed that three coactivator peptides do not have a LXXLL motif but a FXXL(F/Y) motif. Several studies showed that the FXXL(F/Y) motif is preferred by the androgen receptor to interact with coactivators, whereas other NRs show no affinity for peptides with this motif (28–30). Moreover, all six peptides possess a polar residue at the −1 position relative to the coactivator motif (LXXLL). This observation agrees well with previous studies, which showed that a hydrophobic residue is preferred at this position to facilitate proper coactivator binding to various NR LBDs (31, 32). This hydrophobic residue at the −1 position is locked in an aromatic region of RXRα that is induced by the peptide (33). A polar residue at the −1 position is therefore unfavorable.

Peptides that Bind in the Absence of Ligand but Are Not Inducible by 9-*cis* RA

Figure 1, A and B, shows that the remaining 13 peptides equally bind to RXRα with and without 9-*cis* RA. These data suggest that these peptides bind so strongly to the RXRα LBD that this interaction cannot be further enhanced by 9-*cis* RA. This is confirmed by the dose-response curves of one of these peptides [receptor interacting protein (RIP)140_3], shown in Fig. 3A. The estimated K_d^{app} values of the dose-response curves in the absence and presence of 9-*cis* RA are nearly equal (152 nM in the absence and 155 nM in the presence of compound), which indicates that there is no effect on the peptide binding by 9-*cis* RA.

Figure 2B shows the sequence alignment of these 13 strong binding peptides. Except RIP140_3, all peptides contain both the LXXLL motif and the favorable hydrophobic residue at the −1 position (31–33). Obviously, this is one of the essential structural properties that coactivator peptides need: to bind so strongly to the LBD that binding of 9-*cis* RA is no longer required. RIP140_3 is the only peptide without the hydrophobic residue at the −1 position. This suggests that other residues in the coactivator peptide compensate for the absence of the hydrophobic residue. One possible explanation could be the lysine at position 2 that may have a favorable electrostatic interaction with aspartate 295 in the coactivator binding groove. This is corroborated by the observation that the four top-ranked peptides (in the absence of ligand) all contain a positive charge or H-bond donor at position 2 in the coactivator motif.

Peptides Whose Binding Is Inducible by 9-*cis* RA

Finally, there is a set of 17 peptides that weakly or not bind in the absence of ligand and bind (log(MI) >0.30, *i.e*. 2-fold increase in fluorescence intensity) significantly better in the presence of 9-*cis* RA. Some of these peptides have been described in previous studies to interact with RXRα. For example, our observation that RIP140_7 is significantly enhanced in binding to the receptor upon addition of 9-*cis* RA agrees well with a study of Farooqui *et al.* (34). Also the observation that the interaction of SHP_2 with the LBD is enhanced with 9-*cis* RA is in agreement with previous studies (35). Surprisingly, upon addition of the agonist 9-*cis* RA, there is also a significant increase in the affinity of four corepressor peptides [NCoR_3L, silencing mediator of retinoid and thyroid hormone receptor (SMRT)_ID2, PR_H12 and BN2]. To verify the effect of 9-*cis* RA on the affinity of SMRT_ID2, the dose-response curves were measured, and Fig. 3B shows that

A

SWISS-PROT ID	Peptide name	Position	Sequence
NCOA3_HUMAN	SRC3_4	1043-1067	N-Biotinyl- NLEGQSDERALLDQLHTLLSNTDAT -C
NCOA6_HUMAN	ASC2_2	1481-1504	N-Biotinyl- SPAMREAPTSLSQLLDNSGAPNVT -C
NCOA4_HUMAN	ARA70	321-339	N-Biotinyl- SRETSEKFKLLFQSYNVND -C
F. D. PEPT.	Ppt4-1	-	N-Biotinyl- QPKHFTELYFKS -C
NR1H3_HUMAN	LXRa_H12	427-447	N-Biotinyl- ALRLQDKKLPPLLSEIWDVHE -C
SLIM3_HUMAN	FHL2	208-225	N-Biotinyl- YCLNCFCDLYAKKCAGC -C

B

SWISS-PROT ID	Peptide name	Position	Sequence
PRGC1_HUMAN	PGC_1	130-155	N-Biotinyl- DGTPPPQEAEEPSLLKKLLLAPANTQ -C
SHP_HUMAN	SHP_1	9-33	N-Biotinyl- CPCQGAASRPAILYALLSSSLKAVP -C
NCOA3_HUMAN	SRC3_3	724-748	N-Biotinyl- QEQLSPKKKENNALLRYLLDRDDPS -C
NRIP1_HUMAN	RIP140_8	805-831	N-Biotinyl- PVSPQDFSFSKNGLLSRLLRQNQDSYL -C
NCOA2_HUMAN	SRC2_3	732-756	N-Biotinyl- QEPVSPKKKENALLRYLLDKDDTKD -C
NCOA1_HUMAN	SRC1a_4	1421-1441	N-Biotinyl- TSGPQTPQAQQKSLLQQLLTE -C
NRIP1_HUMAN	RIP140_9	922-946	N-Biotinyl- EHRSWARESKSFNVLKQLLLSENCV -C
DAX1_HUMAN	DAX_3_cys	134-159	N-Biotinyl- FCGEDHPRQGSILYSLLTSSKQTHVA -C
NRIP1_HUMAN	RIP140_5	366-390	N-Biotinyl- LERNNIKQAANNSLLLHLLKSQTIP -C
DAX1_HUMAN	DAX_3	136-159	N-Biotinyl- GEDHPRQGSILYSLLTSSKQTHVA -C
NCOA1_HUMAN	SRC1_2	676-700	N-Biotinyl- CPSSHSSLTERHKILHRLLQEGSPS -C
NCOA3_HUMAN	SRC3_2	671-695	N-Biotinyl- SNMHGSLLQEKHRILHKLLQNGNSP -C
NRIP1_HUMAN	RIP140_3	172-196	N-Biotinyl- EKDLRCYGVASSHLKTLLKKSKVKD -C

C

SWISS-PROT ID	Peptide name	Position	Sequence
HAIR_HUMAN	HRCoA_1	552-576	N-Biotinyl- TGLAKHLLSGLGDRLCRLLRREREA -C
Q8N3L6_HUMAN	LCoR	39-63	N-Biotinyl- VTTSPTAATTQNPVLSKLLMADQDS -C
F. D. PEPT.	D47	-	N-Biotinyl- HVYQHPLLLSLLSSEHESG -C
NRIP1_HUMAN	RIP140_6	487-511	N-Biotinyl- SKNSKLNSHQKVTLLQLLLGHKNEE -C
SHP_HUMAN	SHP_2	106-130	N-Biotinyl- TFEVAEAPVPSILKKILLEEPSSSG -C
F. D. PEPT.	C33	-	N-Biotinyl- HVEMHPLLMGLLMESQWGA -C
F. D. PEPT.	D30	-	N-Biotinyl- HPTHSSRLWELLMEATPTM -C
NRIP1_HUMAN	RIP140_1	119-143	N-Biotinyl- MVDSVRKGKQDSTLLASLLQSFSSR -C
NRIP1_HUMAN	RIP140_7	699-723	N-Biotinyl- SGSEIENLLERRTVLQLLLGNPTKG -C
CBP_HUMAN	CBP_1	58-80	N-Biotinyl- NLVPDAASKHKQLSELLRGGSGS -C
NCOA2_HUMAN	SCR2_1S	636-650	N-Biotinyl- KGQTKLLQLLTTKSD -C
ANDR_HUMAN	ARAF1	17-32	N-Biotinyl- KTYRGAFQNLFQSVRE -C
HAIR_HUMAN	HRCoA_2	744-768	N-Biotinyl- AEDRAGRGPLPCPSLCELLASTAVK -C

D

SWISS-PROT ID	Peptide name	Position	Sequence
PRGR_HUMAN	PR_H12	907-933	N-Biotinyl- EMMSEVIAAQLPKILAGMVKPLLFHKK -C
NCOR1_HUMAN	NCoR_3L	2251-2275	N-Biotinyl-GHSFADPASNLGLEDIIRKALMGSF -C
NCOR2_HUMAN	SMRT_ID2	2331-2352	N-Biotinyl- AVQEHASTNMGLEAIIRKALMG -C
F. D. PEPT.	BN2	-	N-Biotinyl- EYHEKRWLEGHIHHRIKSLLENS -C

Fig. 2. Categorization of Peptides Based on the Effect of 9-*cis* RA on their Binding to RXRα LBD

Sequence alignment of A, Coactivator peptides that do not bind to RXRα LBD in the absence of ligand nor in the presence of 10 μM 9-*cis* RA; B, coactivator peptides that equally bind to RXRα LBD in the absence of ligand and in the presence of 10 μM 9-*cis* RA (log(MI) < 0.1) and in addition show a significantly high fluorescence intensity (> 3500); C, coactivator and D, corepressor peptides that show an increase in affinity for the RXRα LBD upon addition of 10 μM 9-*cis* RA [log(MI) > 0.3]. Sequences are aligned manually by their coactivator motifs or corepressor motifs. The amino acids that are part of these motifs are indicated in *bold*. The peptides in panels B and C/D are ordered by increasing fluorescence intensities in the absence and presence of 9-*cis* RA, respectively. P.D. pept., Phage display peptide.

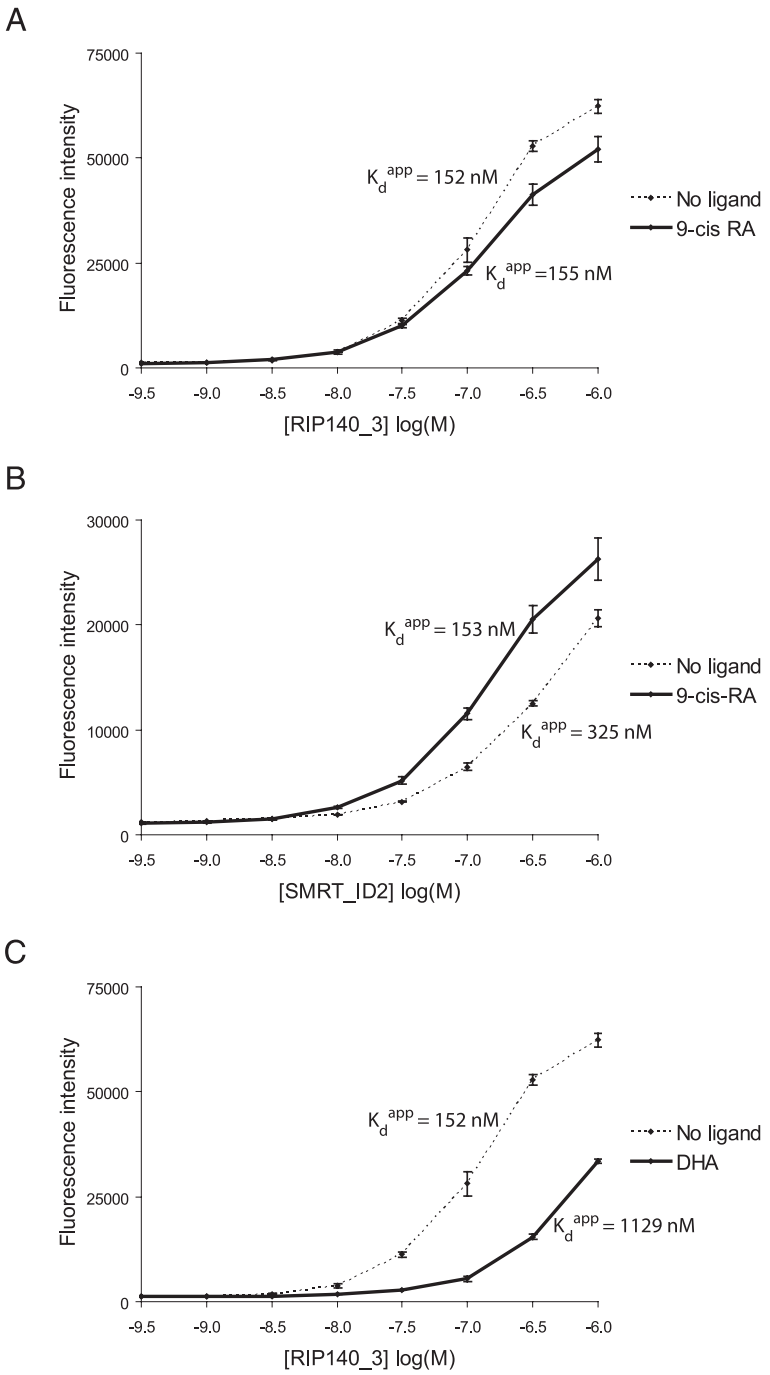

Fig. 3. Peptide Binding Studied by Dose-Response Curves

Ligand-independent (*dashed line*) and ligand-dependent (10 μM, *solid line*) dose-response curves of GST-hRXRα with RIP140_3 and 10 μM 9-*cis* RA (panel A), SMRT_ID2 and 10 μM 9-*cis* RA (panel B), and RIP140_3 and 10 μM DHA (panel C). The SEM value of two separate experiments (each experiment performed in duplicate) is indicated by the *error bars*.

the binding of SMRT_ID2 improves upon addition of 9-*cis* RA, *i.e*. the estimated K_d^{app} changes from 325 to 153 nM. It has been shown before that the second interaction domain of SMRT binds to RXRα in the absence of ligand (36) and that a synthetic agonist LG100268 induces SMRT binding to RXRβ (37). However, for the first time, we demonstrate that the affinity of SMRT_ID2 increases upon addition of the natural agonist, 9-*cis* RA. Similar peptide recruitment data have been described for agonists in peroxisome proliferator-activated receptor (38). From a structural perspective, knowing that H12 adopts the agonist position in all 9-*cis* RA structures (6, 33, 39–41), this leads to the question what the role of this helix is in the

recruitment of the corepressor peptides. The only crystal structure of an NR LBD with a corepressor peptide [SMRT_ID2 (10)] showed that the peptide binds in the coactivator binding groove and that H12 is not in the agonist position. The N-terminal part of SMRT_ID2 relocates H12 toward the N terminus of H3 and partially occupies the agonistic location of H12. The recruitment of both coactivator and corepressor peptides by 9-*cis* RA suggest that 9-*cis* RA induces a conformational change in H12 that is stabilized in the agonist position by coactivator peptides and in the antagonist position by corepressor peptides.

The sequence alignment of the 13 coactivator peptides and the four corepressor peptides that do not bind in the absence of 9-*cis* RA, but do bind significantly better to RXRα in the presence of 9-*cis* RA, are shown in Fig. 2, C and D, respectively. The sequence alignment of the coactivator peptides shows that the residue types at position −1 and 2 are less conserved as compared with the residue types at these positions for peptides that already bind to RXRα in the absence of 9-*cis* RA (Fig. 2B). This suggests that coactivator peptides without a hydrophobic residue at position −1 and without a positively charged or H-bond donating residue at position 2 can only bind to the LBD when H12 is sufficiently stabilized by the ligand. With a sufficiently stable H12, the structural composition of the peptides becomes less critical for binding to the receptor, *i.e*. more sequential variation of the peptides is allowed.

Clustering of Peptide Recruitment Profiles of Various RXRα Ligands

Figure 1B shows the peptide recruitment profiles of a total of 11 different ligands, and 9-*cis* RA is depicted as a reference (*solid black line*). The 10 other ligands include five fatty acids, three synthetic agonists (targretin, LG100268, LG100324), a homodimer antagonist (LG100754), and a RAR agonist TTNPB (Fig. 4). Figure 1B clearly shows that some compounds induce peptide association in a similar manner as 9-*cis* RA,

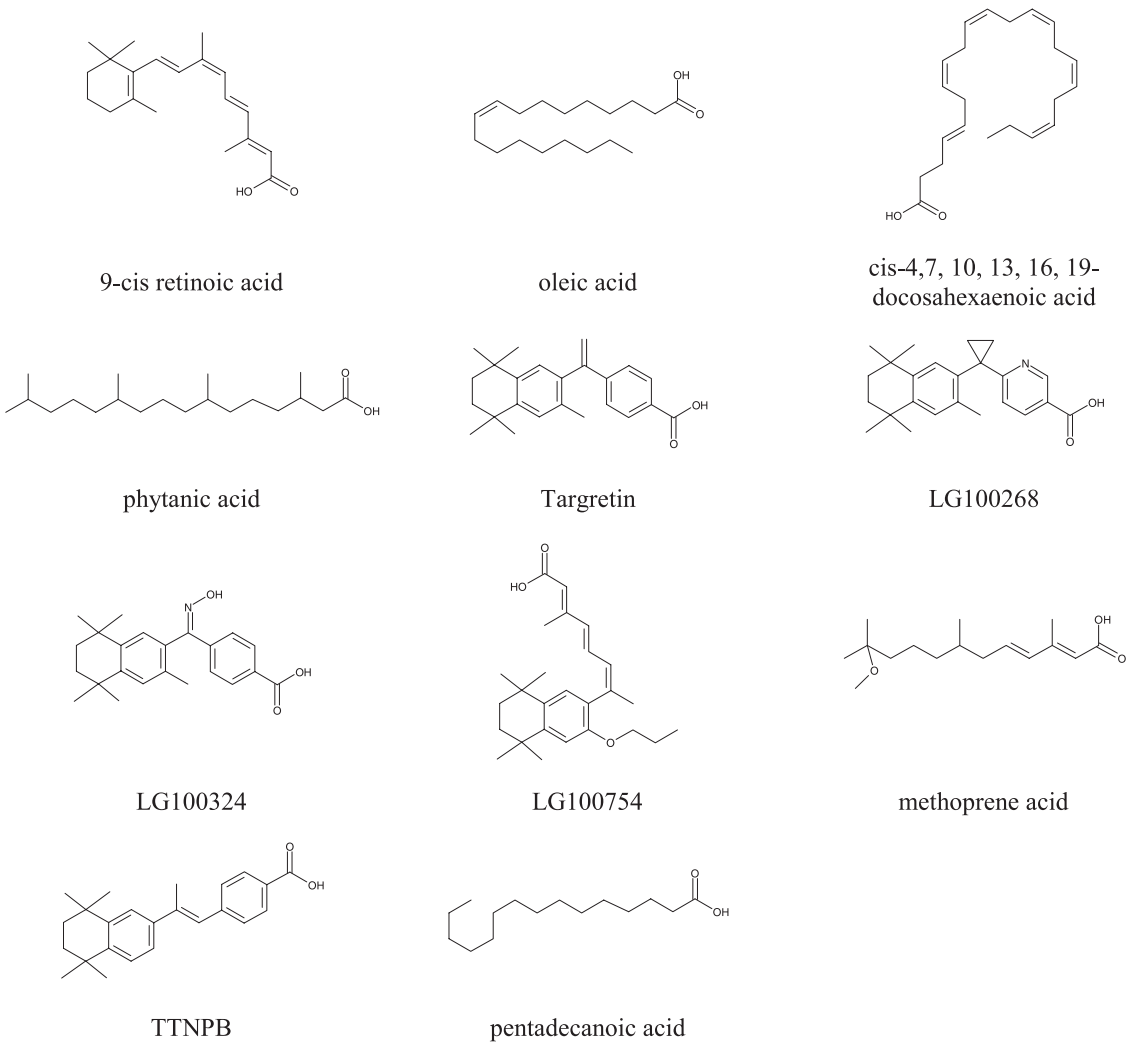

Fig. 4. Chemical Structures of RXR Compounds Used in This Study

whereas other compounds induce peptide dissociation (negative log MI values). Dissociation of peptides is confirmed by dose-response curves. For example, Fig. 3C shows that the estimated K_d^{app} of RIP140_3 increases from 152 nM to 1129 nM upon addition of DHA. This indicates that the firm binding of RIP140_3 in the absence of ligand can be antagonized by a ligand such as DHA. This suggests that DHA destabilized H12 and thereby altered the optimal conditions for coactivator binding.

To identify which compounds induce identical or unique peptide recruitment profiles, we performed a hierarchical clustering (see *Data Analysis* in *Materials and Methods*) on the 11 ligand-induced peptide recruitment profiles (Fig. 5). The dendrogram of the hierarchical clustering of these peptide recruitment profiles was used to determine a boundary to cluster compounds that induce similar peptide recruitment profiles. Figure 6 shows the resulting four different clusters with the corresponding peptide recruitment profiles of the individual compounds in these clusters. On the basis of the shape of the peptide recruitment profiles, we refer to these clusters as a dissociative profile (1), silent profiles (2 and 3), and an associative profile (4).

The natural ligand of RXRα, 9-*cis* RA, clusters together with targretin, LG100268, LG100324, and methoprene acid. These five compounds form the largest cluster (Fig. 6, cluster 4, 9-*cis* RA; *black line*). All compounds in this cluster improve the binding of coactivator and corepressor peptides. The enhancement of the binding of coactivator peptides is in agreement with previous studies, which demonstrate that these compounds act as agonists in RXRα-mediated transcription pathways (18, 42–44). The recruitment of the four corepressor peptides by 9-*cis* RA (see above) is also observed for the other agonists in this cluster.

The second largest cluster contains three compounds that comprise three of the five fatty acids in the ligand set (phytanic acid, oleic acid, and DHA). These fatty acids deteriorate the binding of coactivator peptides and enhance the binding of the corepressor peptides NCoR_3L and, to a lesser extent, SMRT_ID2, indicating that these fatty acids are classical antagonists. However, the corepressor peptide BN2 is dissociated upon binding of these classical antagonists, suggesting that BN2 binds as a coactivator via its IXXLL motif.

The three remaining compounds are in clusters 2 and 3 (Fig. 6). Cluster 2 contains the homodimer antagonist LG100754 and the fatty acid pentadecanoic acid; cluster 3 contains the RARα agonist TTNPB. Compared with the peptide recruitment profiles of the compounds in clusters 1 and 4, these compounds show negligible association or dissociation of most peptides. This raises the question whether these compounds actually bind to the receptor. Pentadecanoic acid binds in the LBP as has been demonstrated by x-ray (45). To determine the binding of LG100754 and TTNPB, we performed a peptide recruitment competition assay with CBP_1 as peptide and 9-*cis* RA as ligand. In the absence of LG100754, the EC_{50} of 9-*cis*

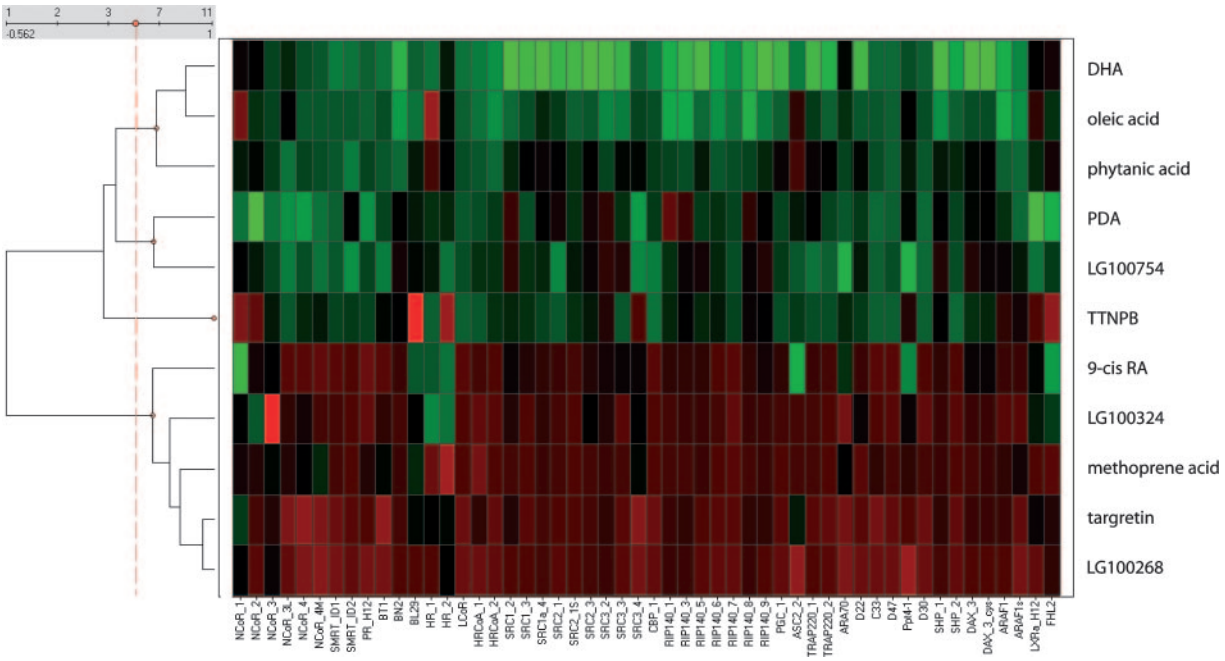

Fig. 5. Hierarchical Clustering of the Peptide Recruitment Profiles of 11 Different RXR Compounds Using a Hierarchical Unweighted Clustering Routine with a Similarity Measure that Was Based on Cosine Correlation

Log(MI) data were normalized. The peptide recruitment profile of each ligand was represented as a row with 52 cells in the distance matrix. Each cell is colored according to the normalized log(MI) value of the peptide with *green* being the highest log(MI) and *red* the lowest log(MI) value. The *vertical red line* indicates the boundary that was chosen to define the separate clusters.

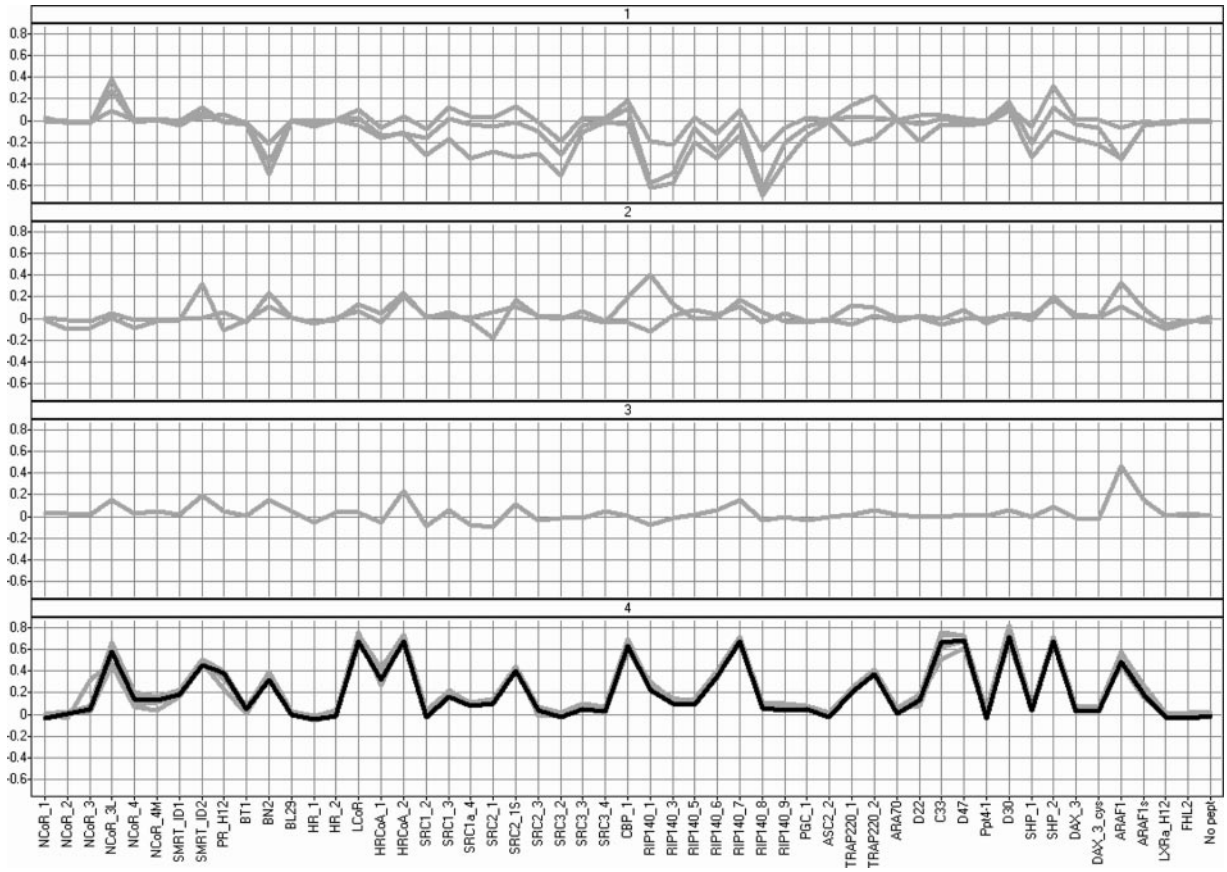

Fig. 6. The Peptide Recruitment Profiles of 11 RXR Compounds Grouped by the Hierarchical Clustering Method (Fig. 5)

Cluster 1 contains oleic acid, phytanic acid, and DHA. Cluster 2 contains PDA and LG100754. Cluster 3 contains TTNPB. Cluster 4 contains 9-*cis* RA, methoprene acid, LG100268, LG100324, and targretin. Each *line* represents the log(MI) values for all peptides for one compound.

RA is 3 nM (Fig. 7A). In the presence of 10^{-7} M LG100754, the EC_{50} is increased to 43 nM, indicating that LG100754 competes with 9-*cis* RA for the same binding site. At even higher concentrations LG100754 (10^{-5} M), 9-*cis* RA is completely substituted by LG100754. These data indicate that LG100754 binds in the LBP but hardly affects the peptide binding profile, *i.e*. the compound does not induce a conformational change in the LBD that results in a significant dissociation or association of peptides.

The same competition assay was performed with TTNPB (Fig. 7B). In the presence of increasing concentrations of TTNPB, the EC_{50} of 9-*cis* RA is hardly changed, indicating that TTNPB does not compete with 9-*cis* RA for the same binding site. Therefore we omitted this compound from further discussion.

Correlation between the Peptide Recruitment Profiles and Ligand Interaction Profiles

To investigate whether there are also differences between the binding modes of ligands, we first analyzed the binding mode of all compounds that have been cocrystallized with human (h)RXRα LBD. These compounds are the natural ligand 9-*cis* RA (6, 33, 39–41), its isomer all-trans retinoic acid (46), the synthetic agonists BMS649 (47) and L79 (48), and two fatty acids, DHA (47) and pentadecanoic acid (PDA) (45). The comparison of different ligand binding modes in RXRα has already been described for BMS649, 9-*cis* RA, and DHA by Egea *et al.* (47). We used a different approach by calculating so-called ligand-receptor interaction profiles, which are believed to represent the binding mode of the ligands. This facilitates the analysis of ligand binding in large sets of crystal structures in an automatic manner. Figure 8 shows the ligand-receptor interaction profiles of the six cocrystallized ligands with 9-*cis* RA highlighted as *solid black line* (see *Materials and Methods* for more details on the methodology to calculate these profiles). The ligand-receptor interaction profile describes the number of contacts between each residue in the LBD and the ligand. Residues in the LBD have been assigned so-called 3D numbers to allow easy comparison of different structures (49). It should be noted that the crystal structures used in this study are derived from multiple independent sources, which could lead to differences in binding modes of the ligand in the LBP

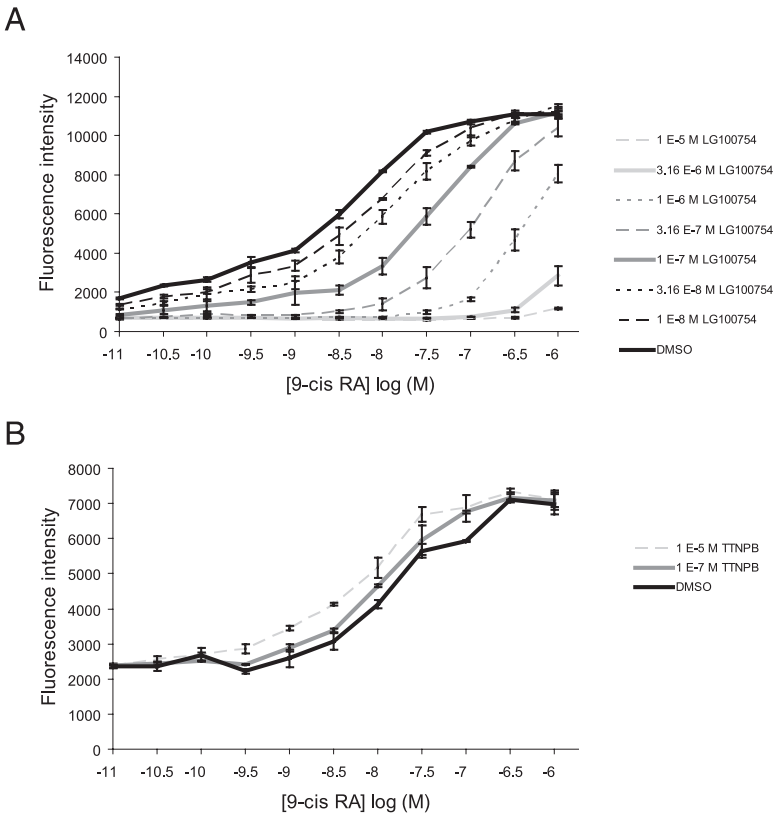

Fig. 7. Competition Studies of LG100754 and TTNPB with 9-*cis* RA

Dose-response curves of 9-*cis* RA were measured in a TR-FRET assay with GST-hRXRα LBD and CBP_1 (0.1 μM) in the presence of increasing concentrations of LG100754 (panel A) and TTNPB (panel B). The SEM of two separate experiments, each performed in duplicate, is indicated by the *error bars*.

in the different crystals. We therefore averaged the contacts between 9-*cis* RA and hRXRα in the five available crystal structures (6, 33, 39–41) and calculated the SE of the average number of contacts in the ligand-receptor interaction profiles (supplemental Fig. 2 published as supplemental data on The Endocrine Society's Journals Online web site at http://mend.endojournals.org). This figure shows that the SE is relatively small, indicating that the binding modes of 9-*cis* RA as resolved from multiple independent sources is highly similar. Figure 8 shows that the six ligands have interactions with residues in H3, H5, the β-sheet, H7,

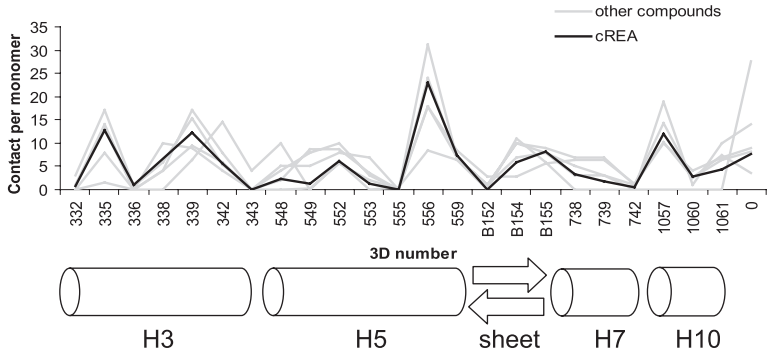

Fig. 8. Ligand-Receptor Interaction Profiles of Compounds in hRXRα Crystal Structures

A ligand-receptor interaction profile describes for each position in the LBD the number of interactions with the ligand. The profile of 9-*cis* RA is highlighted as a *solid black line*. The profiles of the five other compounds that are cocrystallized with hRXRα (all-trans retinoic acid, DHA, PDA, BMS649, and L79) are shown in *light gray*. The secondary structures of the LBD that correspond with the 3D numbers are displayed *below the graph*. The average number of contacts and the SEM in five available crystal structures (6, 33, 39–41) of hRXRα with 9-*cis* RA are given in supplemental Fig. 2.

and H10. The most important ligand binding positions are 335, 339, 556 and 1057, which is in agreement with other members of the NR family (50). The ligand-receptor interaction profiles of the six compounds in Fig. 8 show that the number of contacts between various residues and the ligand differ among the six ligands. This suggests that the ligands have distinct binding modes, which was already described by Egea *et al.* (47) for three of these six ligands. We therefore performed a hierarchical clustering (see *Data Analysis* in *Materials and Methods*) on the six ligand-receptor interaction profiles, which resulted in four different clusters. The corresponding ligand-receptor interaction profiles of the individual compounds in these clusters are shown in Fig. 9.

9-*cis* RA, BMS649, and L79 form the largest cluster (Fig. 9, cluster 4, 9-*cis* RA; *black line*). The compounds in this cluster are described as agonists. BMS649 and L79 are synthetic agonists that better fill the LBP as compared with 9-*cis* RA. The natural ligand only occupies 59% of the total LBP volume (51). One part of the pocket that is not occupied by 9-*cis* RA is near residues at 3D positions 548 and 549 (W305 and N306 in hRXRα, respectively). The synthetic agonists are designed to better fill this side of the pocket, which is reflected in the ligand-receptor interaction profiles that show higher number of contacts between the ligand and positions 549 and 552 (Fig. 9, cluster 4) than that observed in the other clusters.

The three remaining clusters each contain one ligand (Fig. 9, cluster 1–3). Cluster 1 contains all-trans retinoic acid, which is the natural ligand of RAR. The x-ray structure of this compound with RXRα crystallized as a tetramer with H12 of each monomer in the coactivator groove of the adjacent monomer (46). The formation of a tetramer also led to a displacement of the N-terminal part of H3 and the C-terminal part of H10. Therefore, the ligand-receptor interaction profile of this compound is dissimilar to the other profiles. Clusters 2 and 3 both contain a fatty acid, PDA and

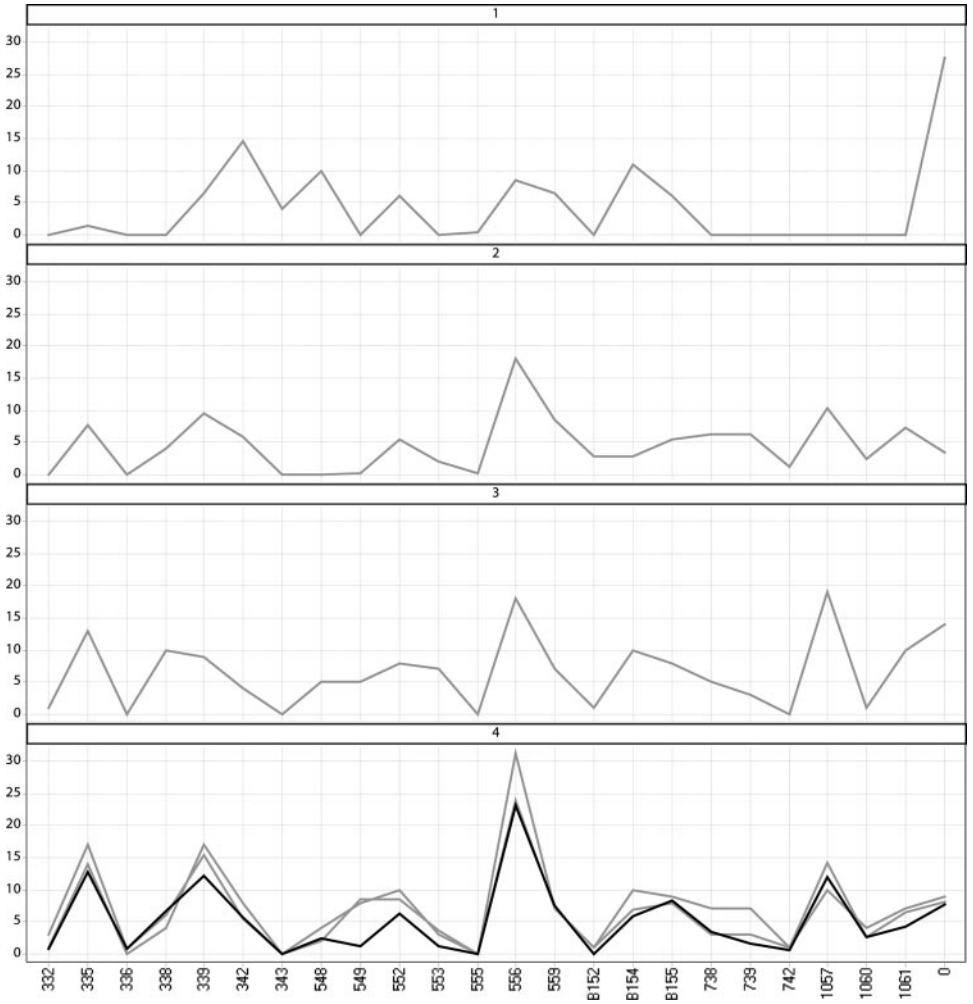

Fig. 9. Ligand-Receptor Interaction Profiles of the Compounds in hRXRα Crystal Structures Grouped by Hierarchical Clustering (Unweighted, Similarity by Correlation)

Cluster 1 contains all-trans-RA. Cluster 2 and 3 contain PDA and DHA, respectively. Cluster 4 contains 9-*cis* RA, BMS649, and L79. Each *line* represents the ligand-receptor interaction profile of a compound.

DHA, respectively. The major difference in the ligand-receptor interaction profile that separates these two clusters is the high number of contacts of DHA (47) with position 1057 (Fig. 9, cluster 3), which is not observed in the ligand-receptor interaction profiles of any other compound. Clustering of the ligand-interaction profiles of these six ligands suggests that there are four different binding modes of RXR compounds in the available crystal structures, which can be detected by this method.

Because the RXRα crystal structure data are limited to six compounds, of which only two are in the peptide recruitment data set, we manually modeled each of the 10 RXRα compounds that were profiled in the peptide recruitment assay and studied the interaction between the receptor and the ligand by MD (see *MD Stimulations of Manually Docked Compounds in the RXRα LBD* in *Materials and Methods*). TTNPB was excluded from the initial set, because this compound does not bind to the RXRα LBD (see above). Figure 10 shows the ligand-receptor interaction profiles that were calculated from model structures of the 10 compounds. To identify how unique or similar the different binding modes of the ligands in the LBP are, we performed the same clustering procedure (see *Data Analysis* in *Materials and Methods*) on the ligand-receptor interaction profiles as was applied to the profiles of the compounds in the crystal structures. From the dendrogram (data not shown) two distinct ligand-receptor interaction profile clusters could be identified. The corresponding profiles of the individual compounds in both clusters are shown in Fig. 11.

The first cluster contains oleic acid, DHA, phytanic acid, PDA, and LG100754. The second cluster contains all agonists: 9-*cis* RA (*black line*), targretin, LG100324, LG100268, and methoprene acid. A clear difference between the two clusters is the number of contacts of the compounds with residues in the C-terminal part of H10, in particular 3D positions 1057 and 1061, which was already observed by Egea *et al.* in comparing the ligand binding modes in crystal structures with 9-*cis* RA, DHA, BMS649, and oleic acid (47). In general, compounds from the agonist cluster have a lower number of contacts with these residues than the compounds in the other cluster. To reveal a structural explanation for the differences in binding mode of compounds from the agonist cluster and the other cluster, we superposed hRXRα crystal structures, each with a compound from one of the clusters (9-*cis* RA from the agonist cluster and DHA from the other cluster; Fig. 12). Figure 12 clearly shows the differences of interaction between each of the two compounds and the H10 region. Although the side chain of cysteine 1057 (corresponding to residue 432 in hRXRα) is in the same orientation in both structures, leucine 1061 (436 in hRXRα) showed a movement of its side chain. In the crystal structure with DHA (47), the side chain of this leucine is shifted toward H12, whereas in the crystal structure with 9-*cis* RA this residue is pointing into the pocket of the LBP. The movement of this side chain toward H12 suggests a destabilization of this helix. This destabilization is reflected in the DHA-induced peptide recruitment profile, which shows a dissociation of most coactivators and confirms destabilization of H12 by interaction of ligands with residue 1061 (436 in hRXRα).

The clustering of the ligand-receptor interaction profiles does not distinguish between compounds that were dissociative (DHA, oleic acid, and phytanic acid) or silent (LG100754 and PDA) in their induced peptide recruitment profiles. We therefore compared the individual ligand-receptor interaction profile of LG100754 with the profiles of representative compounds from the two other clusters (9-*cis* RA for the associative, DHA for the dissociative peptide recruitment cluster; Fig. 11). In addition, the binding mode of LG100754 was compared with that of 9-*cis* RA by superposition of the x-ray RXRα structure with 9-*cis* RA [1FM6 (39)] and the coordinate set of RXRα with LG100754 of the frame with the lowest interaction energy (Fig. 13). Interestingly, the binding mode of LG100754 in the LBP is different from 9-*cis* RA in three areas. The first area is near the tryptophan at position 548 (3D no. 305 in

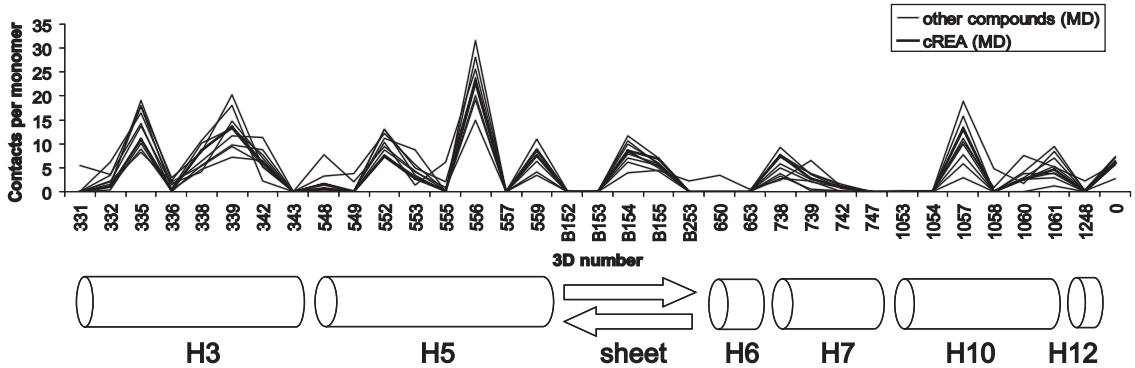

Fig. 10. Ligand-Receptor Interaction Profiles of 10 RXR Compounds that Were Modeled in the hRXRα LBD and Were Tested in the Peptide Recruitment Profiling

TTNPB was excluded from this set because it was shown that it does not bind to the RXRα LBD. The secondary structures of the LBD that correspond with the 3D numbers are displayed *below the graph*.

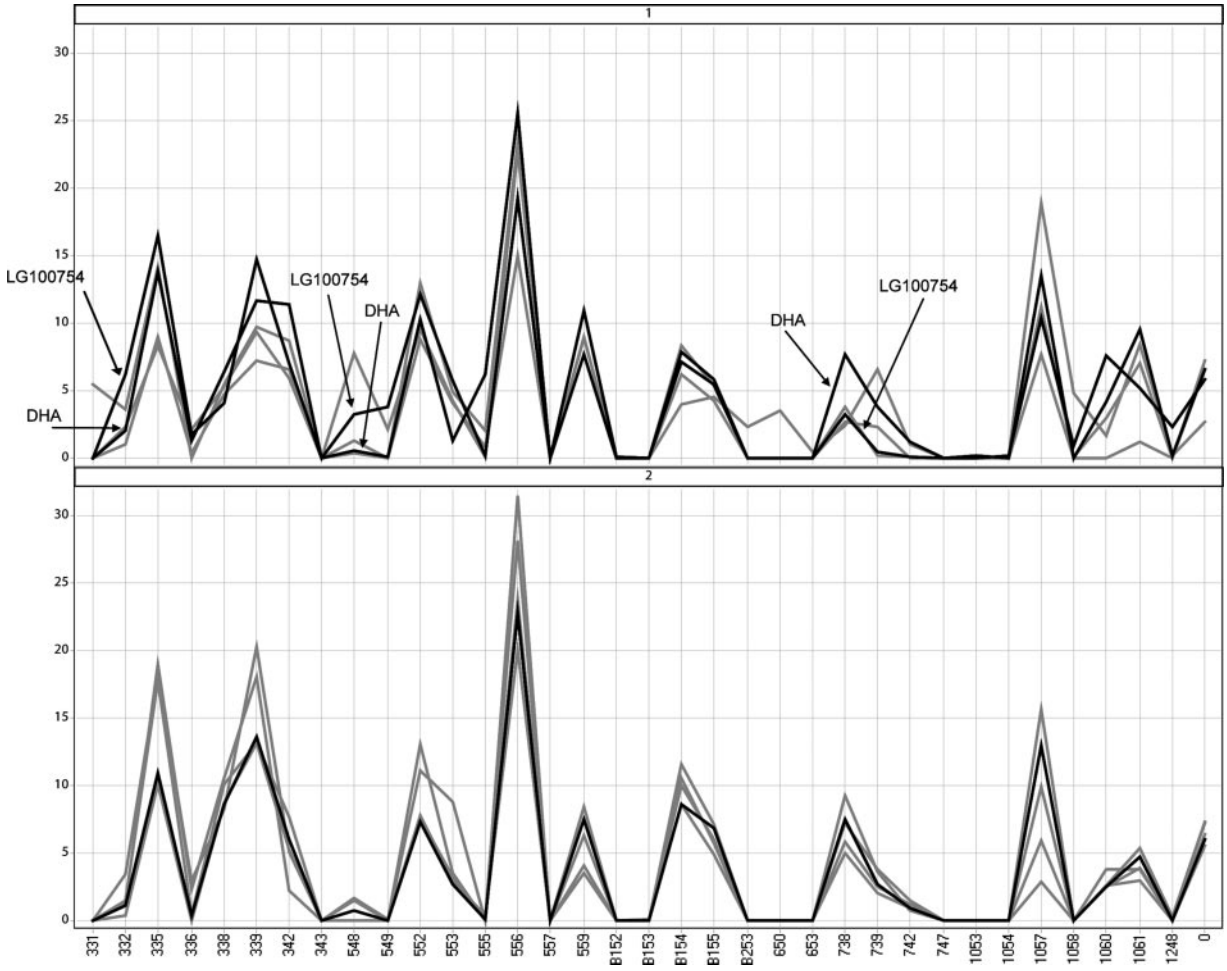

Fig. 11. The Ligand-Receptor Interaction Profiles of 10 RXR Compounds that Were Calculated from the Structures Generated by Molecular Modeling

The profiles were grouped following hierarchical clustering (unweighted, similarity by correlation). Cluster 1 contains oleic acid, DHA (*black line*), phytanic acid, PDA, and LG100754 (*black line*). Cluster 2 contains 9-*cis* RA (*black line*), targretin, LG100324, LG100268, and methoprene acid. Each *line* represents the ligand-receptor interaction profile of a compound. Profiles of DHA and LG100754 are indicated by *arrows*.

hRXRα). The propoxy group of LG100754 points toward this residue, whereas the other ligands do not occupy this space. This leads to a higher number of contacts in the ligand-receptor interaction profile of LG100754 at 3D residue positions 548, 549, 552, and 553 (corresponding to residues 305, 306, 309, and 310 in hRXRα) compared with the profiles of the other two compounds (DHA and 9-*cis* RA, Fig. 11). The second area is in the N-terminal part of H3. The tetra-hydronaphthalene moiety of the homodimer antagonist is shifted toward this part of the LBD, leading to a higher number of contacts with 3D residue positions 331 and 332 (corresponding to residues 264 and 265 in hRXRα). The third area comprises residues in H7. The binding mode of LG100754 shows a lower number of contacts between LG100754 and 3D residue positions 738 and 739 (corresponding to residues 345 and 346 in hRXRα) than 9-*cis* RA and DHA.

DISCUSSION

We hypothesized that the binding mode of a ligand in the LBP determines the conformation at the receptor surface through allosteric coupling. For this purpose, we determined whether compounds that bind differently in the LBP act differently in cofactor recruitment, by comparing the clustering based on ligand-receptor interaction profiles with the clustering of the compounds based on peptide recruitment profiles. We observed two distinct binding modes of ligands in the LBP by means of clustering of the ligand-receptor interaction profiles whereas we observed three distinct conformations of the RXRα LBD by means of clustering of the peptide recruitment profiles. These three distinct conformational changes of the RXRα LBD can be described as an associative, dissociative, or silent peptide recruitment profile. We observed that the five

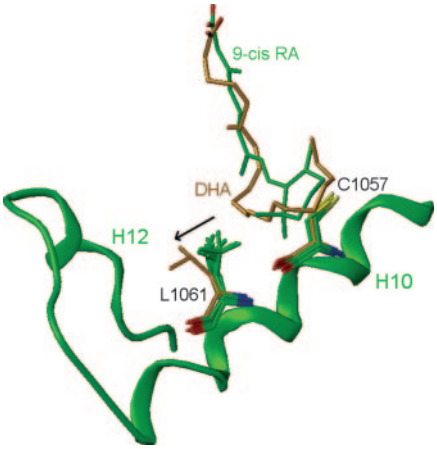

Fig. 12. Comparison of the Binding Modes of DHA (*orange*) and 9-*cis* RA (*green*)

All chains from RXRα crystal structures with 9-*cis* RA (6, 33, 39–41) or DHA (47) were superposed, and the side chains of the cysteines at 3D position 1057 and the leucines at 3D position 1061 are shown. The secondary structure representation is based on the backbone of 1FM6 (39), H10, Helix 10; H12, helix 12.

compounds in the associative peptide recruitment profile cluster are the same five compounds in one of the two clusters of the ligand-receptor interaction profiles. This indicates that there is indeed a correlation between the binding mode of a ligand and the conformation at the surface. However, the ligand-receptor interaction profiles do not yet discriminate between compounds that induce minor conformational changes (silent peptide recruitment profile) and compounds that destabilize H12 (dissociative peptide recruitment profile).

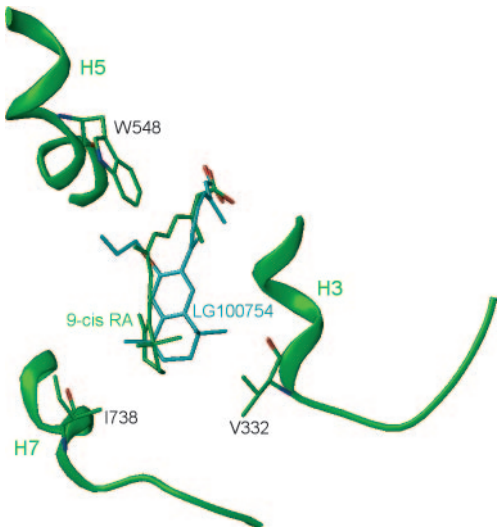

Fig. 13. Comparison of the Binding Modes of LG100754 (*cyan*) and 9-*cis* RA (*green*)

The coordinate set of RXRα with LG100754 of the frame with the lowest interaction energy was superposed on the RXRα crystal structure with 9-*cis* RA (39). The three areas where differences in ligand binding are observed are indicated with one representative residue for each area. The secondary structure representation is based on the backbone of 1FM6 (39). H3, Helix 3; H5, helix 5; H7, helix 7.

In this discussion we will focus on two issues. First, we discuss how well the data from a peptide recruitment assay reflect the effect of a compound in *in vitro* transactivation assays as described in the literature. Second, we give a structural explanation for the three distinct conformational changes at the RXRα surface, *i.e*. the structural mechanism underlying the associative, dissociative, and silent peptide recruitment profile.

Peptide Recruitment Assay *vs. in Vitro* Transactivation Assay

Current models of NR activation suggest that agonist compounds promote the association of a coactivator and the dissociation of a corepressor. Agonist compounds stabilize H12 in an active conformation, thereby facilitating the binding of a coactivator protein and reducing the affinity of corepressors. On the other hand, antagonists displace H12 from the active position, which results in enhancement of the binding of corepressors and reduction of the binding of coactivators. Finally, the so-called selective nuclear receptor modulators (SNRMs) induce such a conformation of H12 that both coactivator and corepressor can bind (52, 53). This may lead to an increase or decrease in gene transcription depending on the concentration of coactivators and corepressors in a cell. In this study, however, the coactivators and corepressors are represented by short peptide fragments, and the ligand-induced recruitment or dissociation of these fragments was measured by peptide recruitment. This raises two questions:

How Well Does a Peptide Recruitment Profile Reflect the Effect of a Compound in a Cell?

We observed that compounds in the associative cluster recruited not only coactivator peptides, but also corepressor peptides. In the context of the above described models for NR activation, our data indicate that 9-*cis* RA and other RXR agonists are not classical agonists, but actually act as SNRMs. The observation that these SNRMs induce coactivator and corepressor binding suggests that these compounds only partially stabilize H12 in the agonist position. This offers H12 sufficient conformational freedom to take the antagonist position in the presence of a corepressor peptide and the agonist position in the presence of a coactivator peptide. The final agonist or antagonist response of the compound in a particular cell type depends on the concentrations of cofactors in this cell type (52, 53). Because several studies have shown that these compounds act as agonists in various cell-based assays (18, 42–44), this suggests that these cell types

have a higher concentration of coactivators than corepressors.

Compounds in the dissociative cluster reduced the binding of coactivator peptides whereas they increased the binding of corepressor peptides, *i.e*. the profile of a typical antagonist. This suggests that these compounds behave as full antagonists in cell-based assays. However, several studies show that fatty acids activate rather than inhibit RXRα-mediated gene transcription (19, 21). One possible explanation is that concentrations of corepressors in these cell-based assays may have been too low to compete with high levels of coactivators and that other cell types with high corepressor concentrations are needed to demonstrate the antagonist activity of fatty acids.

Compounds in the silent cluster did not induce a change in binding affinity for either coactivator or corepressor peptides, suggesting that there will be no change in basal gene transcription. Most likely, these compounds will be silent antagonists due to competition with the natural ligand 9-*cis* RA under physiological conditions.

In general, the correlation between the peptide recruitment profile of a compound and its cellular effect should be carefully interpreted, because it cannot be excluded that the ligand induced a conformational change at other locations at the surface of the LBD that are not detected by means of the current peptide recruitment assay. For example, it has been shown that ligands also induce conformational changes that lead to a different interaction with dimmer partners, which results in a different cellular response (54, 55). We also cannot exclude that peptides in the peptide recruitment profile bind outside the classical coactivator binding groove, as has been suggested to alternative peptide binding positions as has been described for the farnesoid X receptor (56), ERα (57), and Nurr1 (58).

How Well Does the Peptide Recruitment Assay Reflect the Interaction between a Full-Length NR and a Full-Length Cofactor *in Vitro*? In general, we observed that our peptide binding data agree well with the binding data of full-length cofactors that have been described in the literature. For example, the full-length cofactor recruitment of SRC3, FHL2, SRC1, and RIP140 (33, 34, 59, 60) is reflected by the recruitment of peptides derived from these coactivators. In addition, we noticed that the coactivator peptides can be classified as peptides that already strongly bind to the LBD in the absence of an agonist, peptides that only bind in the presence of a ligand, and peptides that do not bind. Peptides with a hydrophobic residue at position −1 in the peptide sequence did already bind strongly to the LBD in the absence of ligand, indicating that these coactivators force H12 in an agonist position, even in the absence of ligand. This suggests that these RXRα-cofactor complexes are continuously active in gene transcription even without ligand.

Peptides that lack a hydrophobic residue at position −1 did bind only to the RXRα LBD in the presence of 9-*cis* RA. This indicates that the cellular action of these coactivators is activated only when 9-*cis* RA is present. This suggests that these coactivators may be more important for ligand-induced gene transcription processes as compared with coactivators that always bind to RXRα. However, binding experiments with full-length cofactors and NRs are needed to study this in more detail.

Peptide Recruitment Profiles and Underlying Structural Mechanisms

Associative and Dissociative Peptide Recruitment Profiles. To determine the structural mechanism underlying the induced association/dissociation of peptides, we focused on compounds that induce an associative peptide recruitment profile and on compounds that induce a dissociative peptide recruitment profile. Comparison of the ligand-receptor interaction profiles of both clusters revealed that the compounds that induce a dissociative peptide recruitment profile have a significant higher number of contacts with residues 1057 and 1061 (3D nos. C432 and L436 in hRXRα, respectively) in the C-terminal part of H10 (47). This suggests that compounds that are in contact with the C terminus of H10 destabilize the agonistic binding mode of H12, resulting in dissociation of coactivators and therefore act as antagonists. A similar mechanism for antagonism has been described for ER (61). The differences in binding of 9-*cis* RA and DHA near the C terminus of H10 were already observed by Egea *et al.* (47), but for the first time we were able to link these structural interactions between ligand and receptor with the ligand-induced association and dissociation of coactivator and corepressor peptides.

Silent Peptide Recruitment Profile. Clustering of the ligand-receptor interaction profiles could not distinguish between compounds that induced a dissociative or silent peptide recruitment profile. However, the proposed ligand binding mode of LG100754 (Fig. 13) shows that there are three plausible explanations for the observation that this compound acts as a silent antagonist.

1) The shift of LG100754 toward H3 excludes a high number of contacts with the C-terminal part of H10, which is needed to destabilize H12 (see above).

2) W548 in H5 is described in stabilizing H12 via a water molecule (6), and therefore the position of this residue is important. Ligands protruding into the area near this residue could disrupt the stabilization of H12, as was already shown by the docking of the retinoid antagonist HX503 (6). The binding mode of LG100754 suggests that the orientation of the propoxy group toward W548 is such that H12 is neither stabilized nor destabilized. This hypothesis is strengthened by the observation that ligands that are identical to LG100754, but have a methoxy or ethoxy group instead of a propoxy group, act as agonists or partial agonists, respectively (54, 55).

3) The N-terminal part of H3 is described in direct

interactions with H12 and the C-terminal part of H11. In addition, an analysis of ligand-receptor contacts in all NR LBDs revealed that partial agonists interact more strongly with this part of H3 (50). LG100754 has a significant higher number of contacts with H3 that could destabilize H12. Together, this suggests that the homodimer antagonist has a unique binding mode, which neither stabilizes nor destabilizes H12 and results in a minor effect on peptide binding in the peptide recruitment assay.

Final Conclusion

In summary, this work shows for one class of compounds that there is a correlation between the binding mode of a ligand (represented by a ligand-receptor interaction profile) and the conformational change it induces at the surface of the RXRα LBD (represented by a peptide recruitment profile). We therefore conclude that clustering of ligand-receptor interaction profiles is a very useful tool to discriminate compounds that may induce different conformations. We also conclude that compounds can be easily classified by their peptide recruitment profiles. However, the translation to a cellular effect is difficult. These peptide recruitment profiles suggest that, depending on the cofactor concentration in the cell, five well-known RXRα agonists actually behave like SNRMs, whereas three weak agonistic fatty acids may act as antagonists and two compounds act as silent antagonists.

We therefore envision that the methods described in this paper can be of great value for drug design. With these methods new compounds can be profiled based on their ligand binding properties and their peptide recruitment properties. Moreover, the combination of both profiles will lead to useful insights in the working mechanism of a NR LBD, which in turn aid the design of compounds with a desired effect.

MATERIALS AND METHODS

Plasmid Construction and Protein Purification

cDNA coding for the ligand-binding domain of human RXRα (hRXRα, amino acids 221–462) was cloned into the *Eco*RI and *XHo*I sites of pGEX-4T-1 (Amersham, Piscataway, NJ). The protein was expressed as a fusion protein with glutathione *S*-transferase (GST) in *Escherichia coli* DH5α and purified by affinity chromatography.

Ligands

Figure 4 shows the structures of the ligands that were used in the peptide recruitment assay. Oleic acid, phytanic acid, DHA, pentadecanoic acid (PDA), methoprene acid, TTNPB, and 9-*cis* RA (all purchased from Sigma-Aldrich) and LG100324, LG100268, LG100754, and targretin (all synthesized in house) were diluted in dimethyl sulfoxide to a final concentration of 10 mM.

Peptides

Supplemental Table 1, published as supplemental data on The Endocrine Society's Online Journals web site, shows the sequences of the 52 N-terminal biotinylated peptides (Neosystem S.A., Strasbourg, France) derived from 15 different cofactors, five NRs, and various phage display peptide libraries (28, 62). Thirty three peptides contain the LXXLL coactivator motif whereas three peptides possess a FXXLF motif and two peptides have a FXXLY motif. Twelve repressor peptides in the set are described by the consensus sequence (L/I/V)XXX(L/I/V)XXX(L/I/V), whereas two repressor peptides (NcoR_4 and NCoR_4M) lack this consensus sequence. Due to similarity between the consensus sequences of a coactivator and corepressor motif, it is possible that some peptides contain both coactivator and corepressor motifs.

TR-FRET Assay

A TR-FRET assay was performed with 52 peptides in the absence and presence of ligand. Each reaction mixture (pH 7.2) contains 50 mM Tris, 50 mM KCl, 1 mM EDTA, 1 mM dithiothreitol, 0.1 mg/ml BSA, 10 nM RXRα LBD, 0.1 μM biotinylated peptide, 10 μM ligand, 8 nM allophycocyanin-labeled Streptavidin (PerkinElmer Life Sciences, Boston, MA), and 1.25 nM LANCE Eu-W1024-labeled anti-GST antibody (PerkinElmer Life Sciences). Each experiment was carried out in duplicate in 384-well plates. Plates were centrifuged and incubated for 24 h at 4 C. Fluorescence at 665 nm was measured on a Victor (Wallac, Inc., Gaithersburg, MD).

To directly visualize the effect of a ligand on recruitment of the different peptides, the MI was calculated, *i.e.* the ratio between the fluorescence intensity in the presence of a ligand and the fluorescence intensity in the absence of ligand. An MI of 2.0 indicates a 2-fold increase of the amount of peptide bound, whereas a MI of 0.5 indicates a 2-fold decrease in the amount of peptide bound. This nonlinear behavior was translated into a linear positive signal for an increase in peptide binding and a linear negative signal for a decrease in peptide binding by calculating the ^{10}log(MI). Log(MI) values above zero indicate recruitment of peptides and thus an associative effect of the ligand on peptide binding. In contrast, negative values indicate dissociation of peptides and therefore a dissociative effect of the compound on peptide binding. A log(MI) value of around zero means that a peptide does not bind and/or that the binding is not changed by the ligand.

To determine the apparent K_d values of specific peptides, the binding curves were determined in a peptide concentration range between 0.1 nM and 1 μM. Calculations were performed in GraphPad Prism (GraphPad Software, Inc., San Diego, CA; nonlinear regression curve fit, one-site binding model). To determine EC_{50} values of ligands, we measured ligand dose-response curves with ligand concentrations ranging from 31.6 pM to 1 μM.

MD Simulations of Manually Docked Compounds in the RXRα LBD

MD simulations were performed using QUANTA/CHARMm (version 31b; Ref. 63) following a protocol that was described previously by Kouwijzer *et al.* (64). The hRXRα LBD of 1FM6 (chain A) was selected as template structure. The initial binding modes of six ligands were obtained from available x-ray structures of either hRXRα or hRXRβ by superposition of the structures onto the template structure. The superposed hRXRα structure with DHA [1MV9 (47)] was used to construct the initial binding mode of phytanic acid, and the superposed hRXRβ structure with LG100268 (37) was used to model LG100754, LG100324, and targretin (supplemental Table 2, published as supplemental data on The Endocrine Society's Online Journals web site). The complexes were protonated, charges were assigned, and ligand atom types and bond

orders were corrected. The MD run started with a heating phase of 10 psec, followed by a 100-psec run at 400 K during which time the coordinate sets were saved every picosecond. These coordinate sets were energy minimized, and for each of these 100 frames the average interaction energy between ligand and protein was calculated. The 10 coordinate sets with the lowest average interaction energy were used to calculate an average ligand-receptor interaction profile.

Ligand-Receptor Interaction Profiles

The number of contacts between ligands and residues in the RXRα LBD was calculated by the Automatic Residue Extraction System (ARES), as was previously described for the analysis of ligand binding in all NR LBDs (50). For each unique receptor-ligand combination, ARES automatically creates a so-called ligand-receptor interaction profile. A contact is included in the profile when the distance between the Van der Waals' surfaces of the atoms of a ligand and a residue is less than 1 Å. A unique number is assigned to each residue position that is structurally conserved within the family of the NR LBDs (49). This 3D number starts with one or two digits that indicate the helix number; similarly B and L reflect residues in the β-sheet and loops, respectively. Residues that are not structurally conserved and therefore do not have a 3D number all got the number zero. Contacts in multiple copies of the same LBD-ligand complex were normalized. If, for example, a LBD-ligand complex is observed two times in one PDB file and three times in another, all contacts in all five chains are summed up and divided by 5.

Data Analysis

The TR-FRET assay and the contact analysis by ARES yielded peptide recruitment profiles and ligand-receptor interaction profiles, respectively. Spotfire DecisionSite (Spotfire, Somerville, MA) was used to cluster both types of profiles by a hierarchical unweighted clustering routine with a similarity measure that was based on (cosine) correlation. Resulting dendrograms were used to determine the boundary to separate clusters.

Acknowledgments

Received February 10, 2006. Accepted October 6, 2006.

Address all correspondence and requests for reprints to: Jacob de Vlieg, Organon NV, Molenstraat 110, P.O. Box 20, 5340 BH Oss, The Netherlands. E-mail: jacob.devlieg@organon.com; or to Simon Folkertsma, Organon NV, Molenstraat 110, P.O. Box 20, 5340 BH Oss, The Netherlands. E-mail: s.folkertsma@cmbi.ru.nl.

S.F. is employed by the Radboud University of Nijmegen. P.I.v.N. is employed by Organon N.V. A.C.F.d.H. was previously employed by Organon N.V. and is employed by Transgenomic Ltd. P.C. is employed by Organon N.V. R.B. was previously employed by Organon N.V. and is employed by Biofocus. A.V. is employed by Organon N.V. G.V. is employed by the Radboud University of Nijmegen. J.d.V. is employed by Organon N.V. and the Radboud University of Nijmegen.

REFERENCES

1. Mangelsdorf DJ, Thummel C, Beato M, Herrlich P, Schutz G, Umesono K, Blumberg B, Kastner P, Mark M, Chambon P, Evans RM 1995 The nuclear receptor superfamily: the second decade. Cell 83:835–839
2. Giguere V 1999 Orphan nuclear receptors: from gene to function. Endocr Rev 20:689–725
3. Kliewer SA, Lehmann JM, Willson TM 1999 Orphan nuclear receptors: shifting endocrinology into reverse. Science 284:757–760
4. Renaud JP, Rochel N, Ruff M, Vivat V, Chambon P, Gronemeyer H, Moras D 1995 Crystal structure of the RAR-γ ligand-binding domain bound to all-trans retinoic acid. Nature 378:681–689
5. Renaud JP, Moras D 2000 Structural studies on nuclear receptors. Cell Mol Life Sci 57:1748–1769
6. Egea PF, Mitschler A, Rochel N, Ruff M, Chambon P, Moras D 2000 Crystal structure of the human RXRα ligand-binding domain bound to its natural ligand: 9-cis retinoic acid. EMBO J 19:2592–2601
7. Darimont BD, Wagner RL, Apriletti JW, Stallcup MR, Kushner PJ, Baxter JD, Fletterick RJ, Yamamoto KR 1998 Structure and specificity of nuclear receptor-coactivator interactions. Genes Dev 12:3343–3356
8. Nolte RT, Wisely GB, Westin S, Cobb JE, Lambert MH, Kurokawa R, Rosenfeld MG, Willson TM, Glass CK, Milburn MV 1998 Ligand binding and co-activator assembly of the peroxisome proliferator-activated receptor-γ. Nature 395:137–143
9. Ding XF, Anderson CM, Ma H, Hong H, Uht RM, Kushner PJ, Stallcup MR 1998 Nuclear receptor-binding sites of coactivators glucocorticoid receptor interacting protein 1 (GRIP1) and steroid receptor coactivator 1 (SRC-1): multiple motifs with different binding specificities. Mol Endocrinol 12:302–313
10. Xu HE, Stanley TB, Montana VG, Lambert MH, Shearer BG, Cobb JE, McKee DD, Galardi CM, Plunket KD, Nolte RT, Parks DJ, Moore JT, Kliewer SA, Willson TM, Stimmel JB 2002 Structural basis for antagonist-mediated recruitment of nuclear co-repressors by PPARα. Nature 415:813–817
11. Perissi V, Staszewski LM, McInerney EM, Kurokawa R, Krones A, Rose DW, Lambert MH, Milburn MV, Glass CK, Rosenfeld MG 1999 Molecular determinants of nuclear receptor-corepressor interaction. Genes Dev 13:3198–3208
12. Hu X, Lazar MA 1999 The CoRNR motif controls the recruitment of corepressors by nuclear hormone receptors. Nature 402:93–96
13. Iannone MA, Simmons CA, Kadwell SH, Svoboda DL, Vanderwall DE, Deng SJ, Consler TG, Shearin J, Gray JG, Pearce KH 2004 Correlation between *in vitro* peptide binding profiles and cellular activities for estrogen receptor-modulating compounds. Mol Endocrinol 18: 1064–1081
14. Downes M, Verdecia MA, Roecker AJ, Hughes R, Hogenesch JB, Kast-Woelbern HR, Bowman ME, Ferrer JL, Anisfeld AM, Edwards PA, Rosenfeld JM, Alvarez JG, Noel JP, Nicolaou KC, Evans RM 2003 A chemical, genetic, and structural analysis of the nuclear bile acid receptor FXR. Mol Cell 11:1079–1092
15. Lee G, Elwood F, McNally J, Weiszmann J, Lindstrom M, Amaral K, Nakamura M, Miao S, Cao P, Learned RM, Chen JL, Li Y 2002 T0070907, a selective ligand for peroxisome proliferator-activated receptor γ, functions as an antagonist of biochemical and cellular activities. J Biol Chem 277:19649–19657
16. Chambon P 1996 A decade of molecular biology of retinoic acid receptors. FASEB J 10:940–954
17. Horton C, Maden M 1995 Endogenous distribution of retinoids during normal development and teratogenesis in the mouse embryo. Dev Dyn 202:312–323
18. Heyman RA, Mangelsdorf DJ, Dyck JA, Stein RB, Eichele G, Evans RM, Thaller C 1992 9-cis Retinoic acid is a high affinity ligand for the retinoid X receptor. Cell 68:397–406
19. Lengqvist J, Mata De Urquiza A, Bergman AC, Willson TM, Sjovall J, Perlmann T, Griffiths WJ 2004 Polyunsaturated fatty acids including docosahexaenoic and ara-

chidonic acid bind to the retinoid X receptor α ligand-binding domain. Mol Cell Proteomics 3:692–703
20. de Urquiza AM, Liu S, Sjoberg M, Zetterstrom RH, Griffiths W, Sjovall J, Perlmann T 2000 Docosahexaenoic acid, a ligand for the retinoid X receptor in mouse brain. Science 290:2140–2144
21. Lemotte PK, Keidel S, Apfel CM 1996 Phytanic acid is a retinoid X receptor ligand. Eur J Biochem 236:328–333
22. Dawson MI 2004 Synthetic retinoids and their nuclear receptors. Curr Med Chem Anti-Canc Agents 4:199–230
23. Li Y, Choi M, Suino K, Kovach A, Daugherty J, Kliewer SA, Xu HE 2005 Structural and biochemical basis for selective repression of the orphan nuclear receptor liver receptor homolog 1 by small heterodimer partner. Proc Natl Acad Sci USA 102:9505–9510
24. Sablin EP, Krylova IN, Fletterick RJ, Ingraham HA 2003 Structural basis for ligand-independent activation of the orphan nuclear receptor LRH-1. Mol Cell 11:1575–1585
25. Watkins RE, Wisely GB, Moore LB, Collins JL, Lambert MH, Williams SP, Willson TM, Kliewer SA, Redinbo MR 2001 The human nuclear xenobiotic receptor PXR: structural determinants of directed promiscuity. Science 292: 2329–2333
26. Uppenberg J, Svensson C, Jaki M, Bertilsson G, Jendeberg L, Berkenstam A 1998 Crystal structure of the ligand binding domain of the human nuclear receptor PPARγ. J Biol Chem 273:31108–31112
27. Xu HE, Lambert MH, Montana VG, Parks DJ, Blanchard SG, Brown PJ, Sternbach DD, Lehmann JM, Wisely GB, Willson TM, Kliewer SA, Milburn MV 1999 Molecular recognition of fatty acids by peroxisome proliferator-activated receptors. Mol Cell 3:397–403
28. Hsu CL, Chen YL, Yeh S, Ting HJ, Hu YC, Lin H, Wang X, Chang C 2003 The use of phage display technique for the isolation of androgen receptor interacting peptides with (F/W)XXL(F/W) and FXXLY new signature motifs. J Biol Chem 278:23691–23698
29. Dubbink HJ, Hersmus R, Verma CS, van der Korput HA, Berrevoets CA, van Tol J, Ziel-van der Made AC, Brinkmann AO, Pike AC, Trapman J 2004 Distinct recognition modes of FXXLF and LXXLL motifs by the androgen receptor. Mol Endocrinol 18:2132–2150
30. He B, Minges JT, Lee LW, Wilson EM 2002 The FXXLF motif mediates androgen receptor-specific interactions with coregulators. J Biol Chem 277:10226–10235
31. Northrop JP, Nguyen D, Piplani S, Olivan SE, Kwan ST, Go NF, Hart CP, Schatz PJ 2000 Selection of estrogen receptor β- and thyroid hormone receptor β-specific coactivator-mimetic peptides using recombinant peptide libraries. Mol Endocrinol 14:605–622
32. Heery DM, Hoare S, Hussain S, Parker MG, Sheppard H 2001 Core LXXLL motif sequences in CREB-binding protein, SRC1, and RIP140 define affinity and selectivity for steroid and retinoid receptors. J Biol Chem 276: 6695–6702
33. Pogenberg V, Guichou JF, Vivat-Hannah V, Kammerer S, Perez E, Germain P, de Lera AR, Gronemeyer H, Royer CA, Bourguet W 2005 Characterization of the interaction between retinoic acid receptor/retinoid X receptor (RAR/RXR) heterodimers and transcriptional coactivators through structural and fluorescence anisotropy studies. J Biol Chem 280:1625–1633
34. Farooqui M, Franco PJ, Thompson J, Kagechika H, Chandraratna RA, Banaszak L, Wei LN 2003 Effects of retinoid ligands on RIP140: molecular interaction with retinoid receptors and biological activity. Biochemistry 42:971–979
35. Seol W, Chung M, Moore DD 1997 Novel receptor interaction and repression domains in the orphan receptor SHP. Mol Cell Biol 17:7126–7131
36. Ghosh JC, Yang X, Zhang A, Lambert MH, Li H, Xu HE, Chen JD 2002 Interactions that determine the assembly of a retinoid X receptor/corepressor complex. Proc Natl Acad Sci USA 99:5842–5847
37. Love JD, Gooch JT, Benko S, Li C, Nagy L, Chatterjee VK, Evans RM, Schwabe JW 2002 The structural basis for the specificity of retinoid-X receptor-selective agonists: new insights into the role of helix H12. J Biol Chem 277:11385–11391
38. Stanley TB, Leesnitzer LM, Montana VG, Galardi CM, Lambert MH, Holt JA, Xu HE, Moore LB, Blanchard SG, Stimmel JB 2003 Subtype specific effects of peroxisome proliferator-activated receptor ligands on corepressor affinity. Biochemistry 42:9278–9287
39. Gampe RT, Jr., Montana VG, Lambert MH, Miller AB, Bledsoe RK, Milburn MV, Kliewer SA, Willson TM, Xu HE 2000 Asymmetry in the PPARγ/RXRα crystal structure reveals the molecular basis of heterodimerization among nuclear receptors. Mol Cell 5:545–555
40. Suino K, Peng L, Reynolds R, Li Y, Cha JY, Repa JJ, Kliewer SA, Xu HE 2004 The nuclear xenobiotic receptor CAR: structural determinants of constitutive activation and heterodimerization. Mol Cell 16:893–905
41. Xu HE, Lambert MH, Montana VG, Plunket KD, Moore LB, Collins JL, Oplinger JA, Kliewer SA, Gampe Jr RT, McKee DD, Moore JT, Willson TM 2001 Structural determinants of ligand binding selectivity between the peroxisome proliferator-activated receptors. Proc Natl Acad Sci USA 98:13919–13924
42. Levin AA, Sturzenbecker LJ, Kazmer S, Bosakowski T, Huselton C, Allenby G, Speck J, Ratzeisen C, Rosenberger M, Lovey A, Grippo JF 1992 9-cis Retinoic acid stereoisomer binds and activates the nuclear receptor RXRα. Nature 355:359–361
43. Boehm MF, Zhang L, Zhi L, McClurg MR, Berger E, Wagoner M, Mais DE, Suto CM, Davies JA, Heyman RA, Nadzam AM 1995 Design and synthesis of potent retinoid X receptor selective ligands that induce apoptosis in leukemia cells. J Med Chem 38:3146–3155
44. Harmon MA, Boehm MF, Heyman RA, Mangelsdorf DJ 1995 Activation of mammalian retinoid X receptors by the insect growth regulator methoprene. Proc Natl Acad Sci USA 92:6157–6160
45. Xu RX, Lambert MH, Wisely BB, Warren EN, Weinert EE, Waitt GM, Williams JD, Collins JL, Moore LB, Willson TM, Moore JT 2004 A structural basis for constitutive activity in the human CAR/RXRα heterodimer. Mol Cell 16: 919–928
46. Gampe Jr RT, Montana VG, Lambert MH, Wisely GB, Milburn MV, Xu HE 2000 Structural basis for autorepression of retinoid X receptor by tetramer formation and the AF-2 helix. Genes Dev 14:2229–2241
47. Egea PF, Mitschler A, Moras D 2002 Molecular recognition of agonist ligands by RXRs. Mol Endocrinol 16: 987–997
48. Haffner CD, Lenhard JM, Miller AB, McDougald DL, Dwornik K, Ittoop OR, Gampe Jr RT, Xu HE, Blanchard S, Montana VG, Consler TG, Bledsoe RK, Ayscue A, Croom D 2004 Structure-based design of potent retinoid X receptor α agonists. J Med Chem 47:2010–2029
49. Folkertsma S, van Noort P, Van Durme J, Joosten HJ, Bettler E, Fleuren W, Oliveira L, Horn F, de Vlieg J, Vriend G 2004 A family-based approach reveals the function of residues in the nuclear receptor ligand-binding domain. J Mol Biol 341:321–335
50. Folkertsma S, van Noort PI, Brandt RF, Bettler E, Vriend G, de Vlieg J 2005 The nuclear receptor ligand-binding domain: a family-based structure analysis. Curr Med Chem 12:1001–1016
51. Otero MP, Torrado A, Pazos Y, Sussman F, De Lera AR 2002 Stereoselective synthesis of annular 9-cis-retinoids and binding characterization to the retinoid X receptor. J Org Chem 67:5876–5882

52. Smith CL, O'Malley BW 2004 Coregulator function: a key to understanding tissue specificity of selective receptor modulators. Endocr Rev 25:45–71
53. Gronemeyer H, Gustafsson JA, Laudet V 2004 Principles for modulation of the nuclear receptor superfamily. Nat Rev Drug Discov 3:950–964
54. Lala DS, Mukherjee R, Schulman IG, Koch SS, Dardashti LJ, Nadzan AM, Croston GE, Evans RM, Heyman RA 1996 Activation of specific RXR heterodimers by an antagonist of RXR homodimers. Nature 383:450–453
55. Canan Koch SS, Dardashti LJ, Hebert JJ, White SK, Croston GE, Flatten KS, Heyman RA, Nadzan AM 1996 Identification of the first retinoid X, receptor homodimer antagonist. J Med Chem 39:3229–3234
56. Mi LZ, Devarakonda S, Harp JM, Han Q, Pellicciari R, Willson TM, Khorasanizadeh S, Rastinejad F 2003 Structural basis for bile acid binding and activation of the nuclear receptor FXR. Mol Cell 11:1093–1100
57. Kong EH, Heldring N, Gustafsson JA, Treuter E, Hubbard RE, Pike AC 2005 Delineation of a unique protein-protein interaction site on the surface of the estrogen receptor. Proc Natl Acad Sci USA 102:3593–3598
58. Codina A, Benoit G, Gooch JT, Neuhaus D, Perlmann T, Schwabe JW 2004 Identification of a novel co-regulator interaction surface on the ligand binding domain of Nurr1 using NMR footprinting. J Biol Chem 279:53338–53345
59. Muller JM, Isele U, Metzger E, Rempel A, Moser M, Pscherer A, Breyer T, Holubarsch C, Buettner R, Schule R 2000 FHL2, a novel tissue-specific coactivator of the androgen receptor. EMBO J 19:359–369
60. Tzameli I, Chua SS, Cheskis B, Moore DD 2003 Complex effects of rexinoids on ligand dependent activation or inhibition of the xenobiotic receptor, CAR. Nucl Recept 1:2
61. Shiau AK, Barstad D, Radek JT, Meyers MJ, Nettles KW, Katzenellenbogen BS, Katzenellenbogen JA, Agard DA, Greene GL 2002 Structural characterization of a subtype-selective ligand reveals a novel mode of estrogen receptor antagonism. Nat Struct Biol 9:359–364
62. Huang HJ, Norris JD, McDonnell DP 2002 Identification of a negative regulatory surface within estrogen receptor α provides evidence in support of a role for corepressors in regulating cellular responses to agonists and antagonists. Mol Endocrinol 16:1778–1792
63. Brooks BR, Bruccoleri RE, Olafson BD, States DJ, Swaminathan S, Karplus M 1983 CHARMM: a program for macromolecular energy, minimization, and dynamics calculations. J Comp Chem 4:187–217
64. Kouwijzer ML, Mestres J 2002 Molecular docking and dynamics simulations in the ligand binding domain of steroid hormone receptors. Trends Drug Res III:57–66

Molecular Endocrinology **is published monthly by The Endocrine Society (http://www.endo-society.org), the foremost professional society serving the endocrine community.**